The Unreasonable effectiveness of effective string theory: The case of the 3D SU(2) Higgs model

Claudio Bonati[1,*] Michele Caselle[2,†] and Silvia Morlacchi[3,‡]

[1]*Dipartimento di Fisica dell'Università di Pisa and INFN, Pisa Largo Pontecorvo 3, I-56127 Pisa, Italy*
[2]*Dipartimento di Fisica dell'Università di Torino and INFN, Turin Via Pietro Giuria 1, I-10125 Turin, Italy*
[3]*Scuola Normale Superiore Piazza dei Cavalieri 7, I-56126 Pisa, Italy*

(Received 21 June 2021; accepted 2 August 2021; published 2 September 2021)

We study string breaking in the three-dimensional SU(2) Higgs model, using values of the gauge coupling for which the confinementlike and Higgs-like regions of the phase diagram are separated just by a smooth crossover. We show that even in the presence of string breaking, the confining part of the interquark potential is well described by the effective string theory and that also the fine details of the effective string, like the higher order terms of the Nambu-Goto action or the boundary correction, can be precisely extracted from the fits and agree with the effective string predictions. We comment on the implications of these results for QCD simulations with dynamical quarks.

DOI: 10.1103/PhysRevD.104.054501

I. INTRODUCTION

A powerful tool to describe the nonperturbative behaviour of the interquark potential in confining gauge theories is the so-called effective string theory (EST) in which the confining flux tube joining together a static quark-antiquark pair is modeled as a thin vibrating string [1–5]. This approach has a long history (for a review see for instance [6–8]) and has been shown to be a highly predictive effective model, whose results can be successfully compared with the most precise existing Monte Carlo simulations in lattice gauge theories (LGTs).

There are two main reasons for the great phenomenological success of this approach. The first is that EST is strongly constrained by the Lorentz symmetry and is thus much more predictive that typical effective theories. The second is that the range of validity of EST is precisely defined (see below for a detailed derivation) and is thus possible to compare EST predictions with numerical data in a controlled and unambiguous way.

The EST description of long flux tubes is perfectly natural to study long distance properties of pure gauge theories, however a major issue in this context is to understand if the EST approach can be extended also beyond pure gauge theories. In view of a possible application to QCD, it would be important to understand which is the fate of the EST description in the presence of dynamical matter fields and thus in a string breaking scenario.

A perfect laboratory to address this issue is the SU(2) Higgs model in three dimensions, which is very similar to real QCD for what concerns string breaking, but at the same time can be simulated at high precision with relatively small effort. The main goal of this paper is to explore the confining potential of the model in the crossover region of the phase diagram between the confining regime and the broken string regime and compare the results of the simulations with the EST predictions. This paper is the natural continuation of the analysis initiated in [9] where, in a model similar to the one discussed here, the shape and size of the confining flux tube was compared with EST predictions.

As we shall see, the confining part of the potential is perfectly described by EST even in its fine details. In particular the contribution due to the higher order terms beyond the Gaussian one contained in the Nambu-Goto action and the so-called boundary term of the EST are in perfect agreement with the data. Moreover we show that if one tries to fit the data neglecting the information coming from the EST action, a wrong value for the string tension (which plays a central role in modeling quarkonia spectra) is obtained. We guess that a similar scenario should occur also in real QCD [10,11] and, in view of the recent efforts to model quarkonia spectra using high precision lattice results [12–15], we stress the importance of the inclusion of EST

*claudio.bonati@unipi.it
†caselle@to.infn.it
‡silvia.morlacchi@sns.it

corrections in the potential models. The role of these corrections will become more and more important as the precision of QCD simulations with dynamical quarks will improve and it will be mandatory to keep them into account for a reliable description of mesonic states in the confining regime of QCD.

This paper is organized as follows: we devote Sec. II to a description of the model and Sec. III to a brief summary of EST results. Our main results are collected in Sec. IV, while Sec. V is devoted to a few concluding remarks.

II. THE MODEL

To study the three-dimensional non-Abelian Higgs model, with gauge group $SU(N_c)$ and N_f scalar fields transforming in the fundamental representation of the gauge group, we can use the following discretization

$$S = -N_f\beta_h \sum_{x,\mu} \mathrm{ReTr}(\varphi_x^\dagger U_{x,\mu}\varphi_{x+\hat{\mu}}) - \frac{\beta}{N_c}\sum_{x,\mu>\nu}\mathrm{ReTr}\Pi_{\mu\nu}(x). \quad (1)$$

Here x denotes a point of a three dimensional isotropic lattice with periodic boundary conditions, $\mu,\nu \in \{0,1,2\}$ labels the lattice directions and $\mathrm{ReTr}\Pi_{\mu\nu}(x)$, with

$$\Pi_{\mu\nu}(x) = [U_\mu(x)U_\nu(x+\hat{\mu})U_\mu^\dagger(x+\hat{\nu})U_\nu^\dagger(x)], \quad (2)$$

denotes the standard Wilson action, i.e., the trace of the product of the link variables around the plaquette in position x laying in the plane (μ,ν). In Eq. (1) $U_{x,\mu}$ is a matrix belonging to the $SU(N_c)$ group while the φ_x fields are $N_c \times N_f$ complex matrices which satisfy the constraint $\mathrm{Tr}\varphi_x^\dagger\varphi_x = 1$.

String breaking is present in this model for any positive value of N_f as soon as[1] $\beta_h > 0$, and in the following we consider the case $N_f = 1$. There are two reasons for this choice: first of all the $N_f = 1$ case is the simplest one from the computational point of view. Moreover in this case it can be rigorously shown that a single thermodynamic phase exists [16,17], while for $N_f > 1$ a global $SU(N_f)$ symmetry is present, which gets spontaneously broken for large enough values of β_h [18,19]. The presence of the phase transition between the $SU(N_f)$ disordered/ordered phases for $N_f > 1$ introduces additional features beyond string breaking, which could hinder the possibility of making contact with real world QCD.

For the sake of the simplicity we study the $N_c = 2$ case, which is the computationally easiest model of this class. For $N_f = 1$ and $N_c = 2$ (and on an infinite lattice) the model in Eq. (1) reduces, in the limit $\beta \to \infty$, to the standard discretization of the nonlinear O(4) σ model, for which a second order phase transition is known to exist at $\beta_h = 0.93586(8)$ [20,21]. *A priori*, for large values of β a line of first order phase transition could be present, which however must end for some $\beta_c > 0$, like in the four-dimensional version of the model (see e.g., [22]). For this reason in the following we explicitly check the absence of phase transitions in the region of the parameter space investigated.

We are interested in the interquark potential $V(R)$ which can be extracted from the correlator of Polyakov loops

$$\langle P(x)P^\dagger(x+R)\rangle \equiv \mathrm{e}^{-N_t V(R)}, \quad (3)$$

as follows:

$$V(R) = -\frac{1}{N_t}\log\langle P(x)P^\dagger(x+R)\rangle, \quad (4)$$

where we set the lattice spacing a to 1 and it will be implied in the following, N_t denotes the lattice size in the compactified time direction and we are studying the system on a cubic lattice with the same size in the spacelike directions (which we shall denote as L) and in the time direction.

The pure gauge limit ($\beta_h = 0$) of the model we consider here has been the subject of several studies in the past [23–31] since it is the simplest LGT with a non-Abelian continuous gauge group and is thus a perfect laboratory to test large distance, nonperturbative, features of these theories.

Similarly, the model in the presence of an external bosonic field ($\beta_h > 0$) has been used a lot in the past to understand and model string breaking. Indeed the choice of bosonic instead of fermionic fields represents an enormous simplification from the numerical point of view, while keeping essentially unchanged the phenomenology of string breaking. Thus one may hope to use models like the one we discuss in this paper as toy models to better understand the string breaking phenomenon in real QCD.

In order to make contact with previous studies in this context [32–36], let us stress that, while in those studies the external field had a self-interaction term of the type $\lambda\phi^4$, in our model the self-interaction term is substituted by the $\mathrm{Tr}\varphi_{\mathbf{x}}^\dagger\varphi_{\mathbf{x}} = 1$ constraint. In this respect we may consider our model as the $\lambda \to \infty$ limit of those studied in the past. This does not change the phenomenology of string breaking but has the advantage of eliminating the λ parameter from the game.

A different strategy to investigate string breaking would be to study the potential, or the flux tube, between static charges in higher representations of the gauge group [9,37–41]. A disadvantage of this kind of approach is

[1]Note that gauge field correlators are symmetric for $\beta_h \to -\beta_h$, as follows from the change of variable $\varphi_x \to (-1)^{x_1+x_2+x_3}\varphi_x$. For this reason we consider just positive values of β_h in the following.

however that there is no way of tuning the physical distance at which string breaking happens, and it could be that ESTs never apply in this case (the precise range of the validity of ESTs will be reviewed in the next section). Using dynamical matter fields in the fundamental representation we can instead vary the physical string breaking length by changing the coupling between matter and gauge fields, i.e., β_h in Eq. (1).

One of the advantages of studying the SU(2) model in $(2+1)$ dimensions is that we can leverage on previous studies to fix the parameters of the model. In particular we can use the scale setting expression obtained in [24]

$$a\sqrt{\sigma} = \frac{1.324(12)}{\beta} + \frac{1.20(11)}{\beta^2} + \mathcal{O}(\beta^{-3}), \tag{5}$$

which is expected to be valid for $\beta \geq 4.5$. Moreover we shall fix in the following $\beta = 9.0$ for which a high precision study of the interquark potential can be found in [25].

As a first step of our analysis we verified that for our choice of β, β_h no phase transition is encountered. To this end we performed for $\beta = 9.0$ a scan in β_h, monitoring the observables

$$E_h = \langle \mathrm{Re}(\varphi_x^\dagger U_{x,\mu} \varphi_{x+\hat{\mu}}) \rangle,$$
$$C_h = L^3 (\langle \mathrm{Re}(\varphi_x^\dagger U_{x,\mu} \varphi_{x+\hat{\mu}})^2 \rangle - E_h^2). \tag{6}$$

This preliminary test showed the absence of phase transitions, as can be seen in Fig. 1, where the values of E_h and C_h are displayed for $L = 32$ and $L = 48$. A peak in the susceptibility C_h is present for $\beta_h \approx 1.04$, which however does not grow/shrinks when increasing the lattice size, and just signals the crossover from the confinementlike to the Higgs-like regions of the phase diagram.

Then, for a selection of values of β_h across the bump shown in Fig. 1, we evaluated the Polyakov loop correlators in the range $1 \leq R \leq 20$ using a 42^3 lattice, and from that the interquark potential $V(R)$. Poyakov loop correlators have been estimated using the multihit [42] and multilevel [43] error reduction techniques. In all the cases the optimal number of hits was around 10 and the optimal configuration for the multilevel was a single level scheme, with temporal slices of 6 lattice spacings. The optimal number of updates to be performed in the multilevel displayed instead some significant dependence on the value of β_f (and obviously on R), going from 16 000 for $R > 12$ at $\beta_h = 0$ to 1000 for $\beta_h = 1.1$ at the same R. For each value of R and β_h a statistics of the order of a few thousands independent draws was accumulated.

Results for $V(R)$ are reported in Table I and are plotted in Fig. 2, from which we see that as β_h increases the string breaking phenomenon in the potential becomes more and more dramatic. In the following sections we shall study in detail this phenomenon and will try to model the rising part of the potential using the effective string approach.

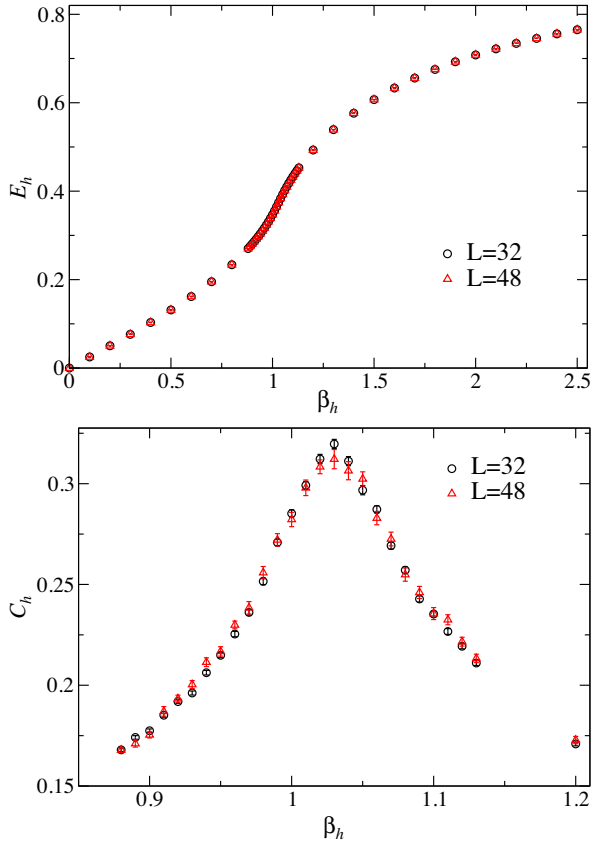

FIG. 1. Dependence of E_h and C_h [defined in Eq. (6)] on β_h for $\beta = 9$. Two different lattice sizes are shown, $L = 32$ and $L = 48$, and no signal of phase transition is present.

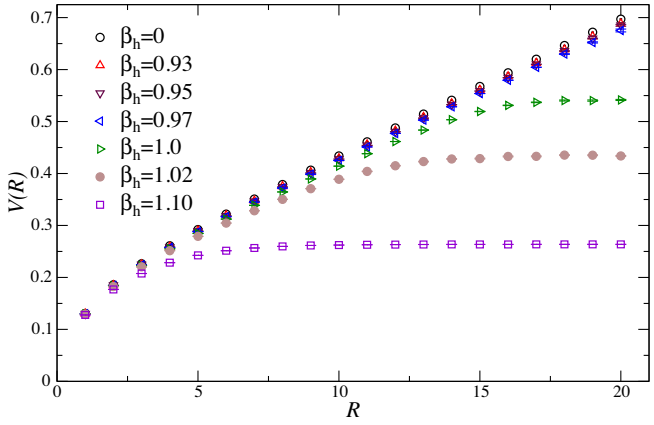

FIG. 2. Static potential computed on a 42^3 lattice at $\beta = 9.0$, for some values of β_h.

III. EFFECTIVE STRING PREDICTIONS

Even if a rigorous proof of quark confinement in Yang-Mills theories is still missing, there is little doubt that confinement is associated to the formation of a thin stringlike flux tube [1–5], which generates, for large quark separations, a linearly rising confining potential.

TABLE I. Values of the static potential (in lattice units) for $\beta = 9.0$ and several β_h, computed on a 42^3 lattice. Note that values corresponding to different Rs are independent from each other, since they have been estimated using different runs.

R	$\beta_h = 0$	$\beta_h = 0.93$	$\beta_h = 0.95$	$\beta_h = 0.97$	$\beta_h = 1.00$	$\beta_h = 1.02$	$\beta_h = 1.1$
1	0.130591(5)	0.130183(2)	0.130096(2)	0.129985(3)	0.129709(3)	0.129415(5)	0.127854(3)
2	0.185930(24)	0.185026(9)	0.184810(8)	0.184482(12)	0.183663(10)	0.182627(16)	0.176884(8)
3	0.226336(54)	0.225036(19)	0.224641(20)	0.224094(29)	0.222498(22)	0.220379(37)	0.207569(10)
4	0.26088(10)	0.258935(12)	0.258390(16)	0.257555(13)	0.255069(16)	0.251504(33)	0.228433(13)
5	0.292121(64)	0.289900(19)	0.289224(26)	0.288047(20)	0.284551(24)	0.279116(56)	0.242479(21)
6	0.321826(94)	0.319235(29)	0.318388(39)	0.316893(29)	0.312243(35)	0.304588(86)	0.251441(29)
7	0.35075(11)	0.347560(32)	0.346559(41)	0.344785(37)	0.338734(39)	0.32833(11)	0.256681(36)
8	0.378806(75)	0.375279(42)	0.374005(56)	0.371982(48)	0.364514(50)	0.35031(17)	0.259691(41)
9	0.406425(98)	0.402511(52)	0.400995(68)	0.398602(62)	0.389540(61)	0.37084(25)	0.261506(37)
10	0.43374(10)	0.429290(63)	0.427730(77)	0.424990(72)	0.414177(65)	0.38892(32)	0.262294(39)
11	0.46088(10)	0.455951(49)	0.454098(62)	0.451205(59)	0.438179(54)	0.40408(44)	0.262873(48)
12	0.48766(10)	0.482307(62)	0.480309(74)	0.477093(72)	0.461537(71)	0.41494(59)	0.263198(49)
13	0.51430(11)	0.508727(86)	0.506574(97)	0.502830(96)	0.48359(10)	0.42295(64)	0.263385(47)
14	0.54099(14)	0.53490(10)	0.53249(12)	0.52847(11)	0.50355(16)	0.42801(70)	0.263563(50)
15	0.56751(16)	0.56067(13)	0.55871(15)	0.55391(13)	0.51934(39)	0.42872(77)	0.263498(49)
16	0.59377(19)	0.58691(17)	0.58445(18)	0.57948(18)	0.53115(49)	0.43282(79)	0.263496(56)
17	0.61988(24)	0.61270(21)	0.61017(24)	0.60444(30)	0.53697(60)	0.43306(81)	0.263646(56)
18	0.64631(36)	0.63865(32)	0.63577(39)	0.62988(53)	0.5405(10)	0.43537(83)	0.263618(56)
19	0.67184(51)	0.66380(48)	0.65982(69)	0.6522(11)	0.5404(12)	0.43517(83)	0.263622(56)
20	0.69700(95)	0.6884(10)	0.6853(17)	0.6752(27)	0.5416(10)	0.43378(86)	0.263646(56)

The simplest example of an EST leading to a linearly rising potential was proposed more than 40 years ago by Lüscher and collaborators [3,4]. They suggested to model the fluctuations of the flux tube in the transverse directions as a free massless bosonic field theory in two dimensions.

$$S[X] = S_{cl} + S_0[X] + \ldots, \tag{7}$$

where the classical action S_{cl} describes the usual perimeter-area term, X denotes the two-dimensional bosonic fields $X_i(\xi_1, \xi_2)$, with $i = 1, 2, \ldots, D-2$, where D is the number of spacetime dimensions (in our case $D = 3$), $D-2$ is the number of transverse directions, ξ_1, ξ_2 are the coordinates on the world sheet, $S_0[X]$ is the Gaussian action

$$S_0[X] = \frac{\sigma}{2} \int d^2\xi (\partial_\alpha X \cdot \partial^\alpha X), \tag{8}$$

and we are assuming an Euclidean signature for both the world sheet and the target space. The fields X_i describe the transverse displacements of the string with respect the configuration of minimal energy.

The Gaussian action can be easily integrated, leading to an explicit expression for the interquark potential, which in the large distance limit is

$$V(R) = \sigma R + c - \frac{\pi(D-2)}{24R} + O(1/R^2), \tag{9}$$

where σ denotes, as usual, the string tension and c is related to the "perimeter" term mentioned above and keeps into account the classical contribution of the Polyakov loops to the potential. We see from the above equation that the effect of the string fluctuations is a correction, known as "Lüscher term," proportional to $1/r$ to the linearly rising potential. This is the first example of an effective string action and, as we shall see below, it is actually nothing else than the large distance limit of the Nambu-Goto string written in the so-called physical gauge.

A. The Nambu-Goto action

A careful inspection shows however that the free bosonic action is not invariant under Lorentz transformations and that further higher order terms must be added to grant invariance. The simplest EST which fulfills Lorentz invariance is the Nambu-Goto action [1,2]:

$$S_{\mathrm{NG}} = \sigma \int_\Sigma d^2\xi \sqrt{g}, \tag{10}$$

where $g \equiv \det g_{\alpha\beta}$ and

$$g_{\alpha\beta} = \partial_\alpha X_\mu \partial_\beta X^\mu \tag{11}$$

is the induced metric on the reference world sheet surface Σ and, as above, we denote the world sheet coordinates as $\xi \equiv (\xi^0, \xi^1)$. This term has a simple geometric interpretation: it measures the area of the surface spanned by the string in the target space and is thus the natural EST realization of the sum over surfaces weighted by their area in the rough phase of the LGT. This model has only one

free parameter: the string tension σ and is thus, as we anticipated, highly predictive.

It is easy to see [6–8] that the free bosonic action of Eq. (8) is the large distance limit of the Nambu-Goto string written in the so-called physical gauge. We report here for completeness the first few terms of the expansion

$$S = S_{\rm cl} + \frac{\sigma}{2}\int d^2\xi\left[\partial_\alpha X_i\cdot\partial^\alpha X^i + \frac{1}{8}(\partial_\alpha X_i\cdot\partial^\alpha X^i)^2 - \frac{1}{4}(\partial_\alpha X_i\cdot\partial_\beta X^i)^2 + \ldots\right]. \tag{12}$$

Despite its apparent complexity the Nambu-Goto action can be integrated exactly in all the geometries which are relevant for LGT: the rectangle (Wilson loop) [44], the cylinder (Polyakov loop correlators) [45,46] and the torus (dual interfaces) [47] leading to a spectrum of states which, in the particular case in which we are interested in this paper, i.e., the correlator of two Polyakov loops is

$$E_n = \sigma R N_t\sqrt{1+\frac{2\pi}{\sigma R^2}\left[-\frac{1}{24}(D-2)+n\right]}. \tag{13}$$

In the large distance limit the spectrum is dominated by the lowest state E_0 from which we may extract the interquark potential

$$V(R) = c + \sigma R\sqrt{1-\frac{\pi(D-2)}{12\sigma R^2}}, \tag{14}$$

and we see, as anticipated, that the Lüscher term of Eq. (9) is nothing else than the first order term of the large distance expansion of the Nambu-Goto potential. From Eq. (14) we may also obtain the domain of validity of the EST approximation, which is given by the value R_c for which the argument of the square root vanishes:

$$R_c = \sqrt{\frac{\pi(D-2)}{12\sigma}}. \tag{15}$$

B. Beyond Nambu Goto: The boundary correction

The Nambu-Goto action is a useful approximation of the "true" EST which describes the nonperturbative regime of LGTs, but it cannot be the exact answer. First, it would predict exactly the same behavior for any confining LGT without dependence on the gauge group. Second, it would predict a mean field exponent for the deconfinement transition in clear contradiction with LGT simulations. It is thus of great theoretical interest to study the terms in the EST action beyond the Nambu-Goto one. The requirement of Lorentz invariance strongly constrains the set of allowed terms. It turns out that the leading correction beyond Nambu Goto is represented by the so-called boundary term.

This term is due to the presence of the Polyakov loops at the boundary of the correlator. The classical contribution associated to this correction is the constant term c which appears in the potential. Beyond this classical term we may find quantum corrections due to the interaction of the Polyakov loop with the flux tube.

The first boundary correction compatible with Lorentz invariance is [48]

$$b_2\int d\xi_0\left[\frac{\partial_0\partial_1 X\cdot\partial_0\partial_1 X}{1+\partial_1 X\cdot\partial_1 X} - \frac{(\partial_0\partial_1 X\cdot\partial_1 X)^2}{(1+\partial_1 X\cdot\partial_1 X)^2}\right], \tag{16}$$

with an arbitrary, nonuniversal coefficient b_2. The lowest order term of the expansion of Eq. (16) is

$$S^{(1)}_{b,2} = b_2\int d\xi_0(\partial_0\partial_1 X)^2. \tag{17}$$

The contribution of this term to the interquark potential was evaluated in [49] using the zeta function regularization:

$$\langle S^{(1)}_{b,2}\rangle = -b_2\frac{\pi^3 N_t}{60R^4}E_4\left(e^{-\frac{\pi N_t}{R}}\right), \tag{18}$$

where E_4 denotes the fourth order Eisenstein series

$$E_4(q) \equiv 1 + \frac{2}{\zeta(-3)}\sum_{n=1}^{\infty}\frac{n^3 q^n}{1-q^n} \sim 1 + 240q + 2160q^2 + \cdots \tag{19}$$

which in the large N_t limit (i.e., $q\to 0$) in which we are interested can be approximated to 1. Thus we see that the boundary term in the EST action essentially amounts to an additional correction proportional to $1/R^4$ to the interquark potential. Looking at Eq. (18) we see that b_2 is a dimensional parameter, with dimensions $[\text{length}]^3$. It is thus customary to rescale it defining a new dimensionless parameter $\tilde{b}_2 \equiv \sqrt{\sigma^3}b_2$

Recent high precision Monte Carlo simulations [28–31,48,50,51] allowed to estimate $\tilde{b}_2$ for a few LGTs. In particular, for the SU(2) model in $(2+1)$ dimensions in which we are interested, one finds $\tilde{b}_2 \sim -0.025$ [28–31].

We end up in this way with the following asymptotic expression for the interquark potential

$$V_{EST}(R) = c + \sigma R\sqrt{1-\frac{\pi(D-2)}{12\sigma R^2}} - \tilde{b}_2\frac{\pi^3}{60\sqrt{\sigma^3}R^4} \tag{20}$$

with three free parameters: c, σ and $\tilde{b}_2$.

IV. RESULTS

A. The pure gauge case: Analysis of the $\beta_h = 0$ data

As a preliminary step test we first studied the static potential in the $\beta_h = 0$ case in which no string breaking is present and compared our results with those of [25] whose simulations were performed at the same $\beta = 9$ value.

We fit the data with Eq. (20) keeping c, σ and $\tilde{b}_2$ as free parameters in the range $R_{\min} \le R \le R_{\max}$. We studied different values of $R_{\min}$ in the range $3 \le R_{\min} \le 12$ and fixed[2] $R_{\max} = 20$. We also performed a set of fits in the same range using the Cornell form of the potential

$$V_{\text{Cornell}}(r) = c + \sigma R - \frac{k_L \pi}{24 R}, \tag{21}$$

keeping c, σ and k_L as free parameters. This expression coincides with the free bosonic potential Eq. (9) when $k_L = 1$ and allows us to test the improvement of the Nambu-Goto action with respect to the free bosonic approximation in describing the data.

Results of the fits are reported in Figs. 3 and 4 and, for the EST potential, in Table II. In order to give a feeling of the magnitude of the boundary term, we report in the table the coefficient κ_B of the $1/R^4$ correction in the potential instead of $\tilde{b}_2$, with

$$\kappa_B \equiv -\tilde{b}_2 \frac{\pi^3}{60\sqrt{\sigma^3}}. \tag{22}$$

Looking at these data we see a few interesting results:

(i) Inserting in the expression for R_c [see Eq. (15)] the best fit value of σ we find $R_c \sim 3.2$, thus the range of validity of the EST potential is for $R \ge R_{\min} = 4$. Remarkably enough we find a very good χ^2 using all the data within the range of validity of EST. Moreover if we try to add also $R = 3$ we have a jump in the χ^2 (which is also associated with a jump in the value of σ). Notice also the remarkable stability of this result for different choices of $R_{\min}$. As a final result, taking into account the systematics connected to the choice of the fit range, we report $\sigma = 0.02583(3)$ (shown also in Fig. 3).

(ii) The value of σ that we find is compatible with the scale setting result $\sigma = 0.0262(8)$ of Eq. (5). It slightly disagrees with the estimate of [25]: $\sigma = 0.02590(1)$ which however was obtained without keeping into account the boundary correction which,

[2]We also performed a set of fits varying $R_{\max}$ in order to test for the possible presence of finite size effects. We verified that (with the exception of the data at $\beta_h = 0.95$ which we shall discuss in detail below) there was no signature of finite size corrections and in the following we shall only report the results for $R_{\max} = 20$.

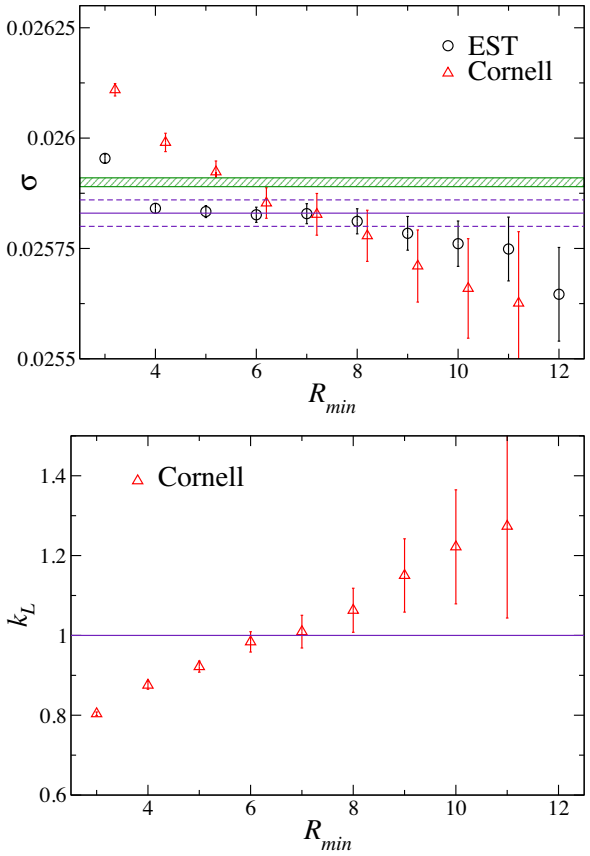

FIG. 3. Estimates of σ (upper panel) and of the Luscher term (lower panel) for several fitting ranges (data up to 20 lattice spacings included) for the case $\beta = 9.0$, $\beta_h = 0$, $L = 42$. As our final estimate for the string tension we take $\sigma = 0.02583(3)$, which is also indicated by the horizontal strip. The horizontal green band corresponds to the result reported in [25], obtained without taking into account the boundary contribution to the potential.

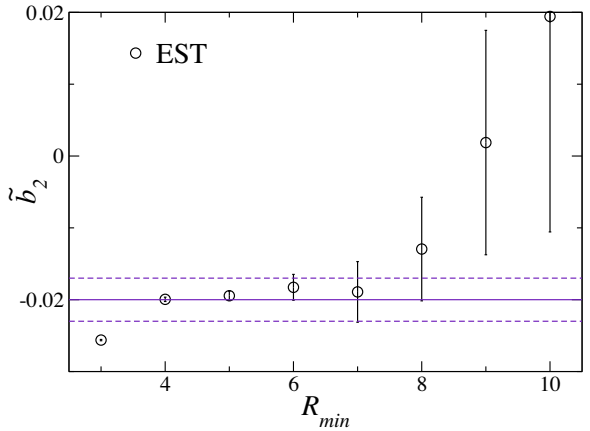

FIG. 4. Estimates of the coefficient $\tilde{b}_2$ of the boundary term in V_{est} for $\beta_h = 0$ (data up to 20 included). We report $\tilde{b}_2 = -0.020(3)$ as our final estimate.

TABLE II. Results of the fit of the $\beta_h = 0$ data to the V_{EST} potential for various values of $R_{\min}$ and $R_{\max} = 20$. κ_B is defined in Eq. (22).

$R_{\min}$	σ	c	κ_B	χ^2/dof	dof
3	0.0259540(93)	0.187083(94)	3.1670(92)	25.9	15
4	0.025841(11)	0.18854(10)	2.482(30)	0.70	14
5	0.025834(14)	0.18863(16)	2.421(76)	0.69	13
6	0.025826(17)	0.18873(22)	2.28(22)	0.70	12
7	0.025829(23)	0.18870(31)	2.35(52)	0.77	11
8	0.025811(28)	0.18896(40)	1.61(90)	0.74	10
9	0.025784(38)	0.18941(58)	−0.2(1.9)	0.69	9
10	0.025761(51)	0.18981(82)	−2.4(3.8)	0.72	8
11	0.025749(72)	0.1900(12)	−3.9(7.3)	0.82	7
12	0.02565(11)	0.1919(16)	−20(14)	0.66	6

as we shall see below, is mandatory to correctly fit the data.

(iii) The inclusion of the boundary correction turns out to be mandatory to fit the data down to $R_{\min} = 4$. Any attempt to fit the data without it leads to unacceptable values of the reduced χ^2 for $R_{\min} = 4$. The relevance of the boundary term decreases as we increase $R_{\min}$ and becomes negligible starting from $R_{\min} = 8$, a result which could have been anticipated by a direct evaluation of the size of the correction. Moreover we see, looking at Fig. 4 that in the range $4 \le R_{\min} \le 8$ our estimate of $\tilde{b}_2$ is very stable, and keeping into account the systematic uncertainties of the fit we may quote as our final result $\tilde{b}_2 \sim -0.020(3)$ which is fully compatible with the one obtained by Brandt $\tilde{b}_2 \sim -0.025(5)$ [28–31].

It is very interesting to compare these results with those obtained with the Cornell potential of Eq. (21). Looking at Fig. 3 we see that the string tension shows a clear trend to decrease as $R_{\min}$ increases and at the same time the coefficient of the Lüscher term, which for $R_{\min} = 4$ is ≈10% below the correct result, increases with $R_{\min}$. The results of the fits stabilize around $R_{\min} = 8$, a value for which higher order corrections beyond the Gaussian term become negligible. We learn from this analysis that for small values of R both the boundary term and the higher order corrections of the Nambu-Goto action are mandatory to fit the data, that they have a comparable size and thus must both be included in the fit.

B. String breaking: Analysis of the $\beta_h \neq 0$ data

Looking at Fig. 2 we see that for the first three values of β_h the shape of the potential is very similar to the unperturbed one. This suggests trying the same fitting function V_{EST} also for these cases. In the $\beta_h = 0.93$ case this works perfectly, with a reduced $\chi^2 = 0.85$ in the whole range $4 \le R \le 20$ and best fit values for the parameters with a statistical uncertainty similar to that of the unperturbed ones (see the second line of Table III). However, already for the next value of β_h the same procedure no longer works, meaning that, even if they are not visible in the plot, the effects of string breaking are already affecting the large distance behavior of the potential. For $\beta_h = 0.95$ we can still control these deviations by cutting the fit to the value $R_{\max} = 14$ and we find again values of the parameters similar to the unperturbed ones (see the third line of Table III), but this is no longer possible for the subsequent values.

We may address the string breaking phenomenon, following [34–36], assuming a mixture of a "string state" described by $V_{EST}(R)$ and a "broken string state" $E_{sb}(R)$ (for a different approach see e.g., [52,53]). The simplest way to model this mixture is by diagonalizing the 2×2 matrix

$$\begin{pmatrix} V_{EST}(R) & M(R) \\ M(R) & E_{sb}(R) \end{pmatrix}, \tag{23}$$

where $V_{EST}(R)$ is the energy of the "string state," $M(R)$ is a mixing term (*a priori* dependent on R) and $E_{sb}(R)$ is the energy of the "broken string state." We shall assume in the following, as a first approximation, that both M and E_{sb} have a negligible dependence on R and shall take them as constants (we shall comment on this approximation at the end of this section).

The eigenvalues of the mixing matrix are

$$V_{\pm}(R) = \frac{V_{EST}(R) + E_{sb} \pm \sqrt{(V_{EST}(R) - E_{sb})^2 + 4M^2}}{2} \tag{24}$$

with the fundamental state, the one that we observe in our simulations, being associated to the minus sign. We thus fitted the Polyakov loop correlators with the "string breaking potential" $V_{sb}(R)$

TABLE III. Results of the fit with the V_{sb} potential for various values of β_h and the choices of $R_{\min}$ and $R_{\max}$ discussed in the text.

β_h	σ	c	κ_B	M	E_{sb}	χ^2/dof	dof
0	0.025841(11)	0.18854(10)	2.482(30)			0.70	14
0.93	0.0254058(56)	0.188492(50)	2.5121(80)			0.85	14
0.95	0.0252119(81)	0.188815(71)	2.515(11)			0.86	8
0.97	0.024941(15)	0.189111(55)	2.5828(94)	0.0081(21)	0.6836(91)	0.75	12
1.00	0.023842(36)	0.19380(19)	2.456(59)	0.02541(55)	0.54818(69)	1.04	11
1.02	0.02172(27)	0.2042(14)	1.77(27)	0.0312(14)	0.44064(70)	1.34	11

$$V_{sb}(R) = \frac{V_{EST}(R) + E_{sb} - \sqrt{(V_{EST}(R) - E_{sb})^2 + 4M^2}}{2} \tag{25}$$

with five degrees of freedom: the three parameters contained in V_{EST}: c, σ and κ_B and the two new parameters M and E_{sb}. Despite the large number of free parameters the fits turned out to be very stable for all the values of β_h that we studied, with good χ^2 values in the whole range $4 \leq R \leq 20$ for $\beta_h = 0.97$ and in the range $5 \leq R \leq 20$ for $\beta_h = 1.00$ and 1.02. For these values of β_h, including in the fit also the point at $R = 4$ led to values of the reduced $\chi^2 \sim 2$.

By exploring the parameter space in the vicinity of the best fit values reported in Table III, we realized that they correspond to very deep and narrow minima in the parameter space and this probably explains the stability of the fits. To better asses the reliability of the fitting procedure we also fixed one of the parameters to its 1σ-deviation value, checking the stability of the remaining parameters, whose variations are taken as estimators of the systematics. In this way we get the for the three relevant physical quantities σ, $\tilde{b}_2$ and E_{sb} the results reported in Table IV. For $\beta \geq 0.97$ the errors quoted in Table IV for σ and E_{sb} are dominated by the uncertainty on the mixing parameters M. The error on $\tilde{b}_2$ is instead dominated by the value of $R_{\min}$ chosen in the fit and we estimated it combining the values obtained up to $R_{\min} = 6$.

Following [34] we can extract from the results of the fit a rough estimate of the "string breaking threshold" R_{sb} defined as the value of R for which the extrapolation of V_{EST} crosses E_{sb}. We report these values in the last column of Table IV. For $\beta_h = 1.10$ we could not perform the analysis since we have too few values of R before the string breaking threshold.

A few comments are in order on these results:

(i) As β_h increases the string breaking scale R_{sb} decreases and will eventually become smaller than the critical radius R_c of EST. When $R_{sb} < R_c$ we obviously do not expect an EST regime at short distance. Looking at our data (see Fig. 2) this threshold in β_h seems to be reached at $\beta_h = 1.10$ for which $R_{sb} \sim 4$. Beyond this value we may consider the string breaking process to be completed.

(ii) It is interesting to see that for $\beta_h = 0.97$ (for which $R_{sb} \sim 20$) looking at the data apparently there seems to be no evidence of string breaking (see Fig. 2); however we have seen from the above analysis that this impression is wrong and that, without keeping into account the mixing with the E_{sb} term, it would be impossible to fit the data (even if the string breaking threshold is larger than the set of data included in the fit).

(iii) The string tension shows a smooth decreasing trend as β_h increases. This trend is small in magnitude, but definitely larger than the uncertainties. It can be used to construct lines of "constant physics" in the (β, β_h) phase diagram. These lines almost (but not exactly) coincide with vertical lines ($\beta = \text{const}$). The value of the boundary term is almost constant within the errors along the whole line and agrees with the estimate obtained by Brandt in the $\beta_h = 0$ case.

(iv) As we mentioned above for $\beta_h = 1.00$ and 1.02 including in the fit also the point at $R = 4$ led to an increase in the values of the reduced χ^2. This small deviation of the $R = 4$ value with respect to the EST prediction could be the signature of a short distance dependence of E_{sb} on R. Indeed it is conceivable to have in the broken string potential a massive excitation which would show up in a term of the type

$$E_{sb}(R) = E_{sb} + Ae^{-mR}. \tag{26}$$

Unfortunately, the range of our data does not allow us to extract such a massive excitation, which however could become visible performing simulations at a larger value β, with a smaller value of the lattice spacing.

TABLE IV. Best fit estimates for σ, $\tilde{b}$ and E_{sb} for various values of β_h. The quoted uncertainties keep into account various systematic effects in the fits, as discussed in the text. Note that the error on E_{sb} for $\beta_h = 0.97$ is quite asymmetric, likely due to the fact that R_{sb} is just on the boundary of the fit range.

β_h	σ	$\tilde{b}_2$	E_{sb}	R_{sb}
0	0.02583(3)	0.020(3)		
0.93	0.02541(1)	0.019(2)		
0.95	0.02523(3)	0.019(3)		
0.97	0.02493(3)	0.020(1)	$0.683^{+0.018}_{-0.009}$	~20
1.00	0.02386(8)	0.019(3)	0.548(2)	~15
1.02	0.0214(8)	0.006(15)	0.440(2)	~10.5

We conclude this section with a few comments on the R independence of the entries $M(R)$ and $E_{sb}(R)$ of the mixing matrix in Eq. (23). While it is natural to expect the R dependence of these terms to be weaker than the one in $V_{EST}(R)$, the fact that our data are perfectly reproduced by completely neglecting this dependence could seem surprising and, maybe, an indication that the model studied is somehow pathological. It is thus reassuring that the same is true also for the case of QCD studied in Ref. [11], where however only the linearly rising part of $V_{EST}(R)$ was used to fit the data. To unambiguously identify the R dependence of $M(R)$ and $E_{sb}(R)$ much higher accuracy seems to be required, likely together with a careful investigation of the excited states.

V. CONCLUDING REMARKS

As we have seen, the formalism of the mixing matrix allows to disentangle in a clean and precise way the string

breaking potential from the confining one and allows to study fine details of both potentials. Remarkably enough, the EST picture seems to describe well the data even in presence of string breaking. In particular, the boundary term and the higher order terms beyond the gaussian one in the Nambu-Goto action seem not to be affected by the string breaking and are clearly visible in the fits.

This is particularly important since, as we have seen, when string breaking occurs the confining potential can be studied only at short distance, below the string breaking threshold, and it is exactly in this regime that higher order terms of the EST like the next to gaussian terms of the Nambu-Goto action and the boundary term, become particularly important and cannot be neglected. The fits performed with the Gaussian term only (see Fig. 3) show that neglecting these corrections would lead to a wrong estimate of the string tension (and of the Luscher term itself). We think that this is an important lesson to keep in mind when looking at the interquark potential in QCD for which the string breaking scale is of the same size of the intermediate values of β_h that we studied in this paper. Since we are by now entering the precision era of lattice simulations for phenomenology [11–13], this type of correction will become more and more important and should be kept into account to reach the correct phenomenological estimates of the interquark potential.

ACKNOWLEDGMENTS

Numerical simulations have been performed on the CSN4 cluster of the Scientific Computing Center at INFN-PISA.

[1] Y. Nambu, Phys. Rev. D **10**, 4262 (1974).
[2] T. Goto, Prog. Theor. Phys. **46**, 1560 (1971).
[3] M. Luscher, Nucl. Phys. **B180**, 317 (1981).
[4] M. Luscher, K. Symanzik, and P. Weisz, Nucl. Phys. **B173**, 365 (1980).
[5] J. Polchinski and A. Strominger, Phys. Rev. Lett. **67**, 1681 (1991).
[6] O. Aharony and Z. Komargodski, J. High Energy Phys. 05 (2013) 118.
[7] B. B. Brandt and M. Meineri, Int. J. Mod. Phys. A **31**, 1643001 (2016).
[8] M. Caselle, Universe **7**, 170 (2021).
[9] C. Bonati and S. Morlacchi, Phys. Rev. D **101**, 094506 (2020).
[10] G. S. Bali, H. Neff, T. Duessel, T. Lippert, and K. Schilling (SESAM Collaboration), Phys. Rev. D **71**, 114513 (2005).
[11] J. Bulava, B. Hörz, F. Knechtli, V. Koch, G. Moir, C. Morningstar, and M. Peardon, Phys. Lett. B **793**, 493 (2019).
[12] P. Bicudo, M. Cardoso, N. Cardoso, and M. Wagner, Phys. Rev. D **101**, 034503 (2020).
[13] P. Bicudo, N. Cardoso, L. Müller, and M. Wagner, Phys. Rev. D **103**, 074507 (2021).
[14] R. Bruschini and P. González, Phys. Rev. D **102**, 074002 (2020).
[15] R. Bruschini and P. González, Phys. Rev. D **103**, 114016 (2021).
[16] K. Osterwalder and E. Seiler, Ann. Phys. (N.Y.) **110**, 440 (1978).
[17] E. H. Fradkin and S. H. Shenker, Phys. Rev. D **19**, 3682 (1979).
[18] C. Bonati, A. Pelissetto, and E. Vicari, Phys. Rev. Lett. **123**, 232002 (2019).
[19] C. Bonati, A. Pelissetto, and E. Vicari, Phys. Rev. D **101**, 034505 (2020).
[20] M. Campostrini, A. Pelissetto, P. Rossi, and E. Vicari, Nucl. Phys. **B459**, 207 (1996).
[21] H. G. Ballesteros, L. A. Fernandez, V. Martin-Mayor, and A. Munoz Sudupe, Phys. Lett. B **387**, 125 (1996).
[22] C. Bonati, G. Cossu, M. D'Elia, and A. Di Giacomo, Nucl. Phys. **B828**, 390 (2010).
[23] J. Ambjorn, P. Olesen, and C. Peterson, Phys. Lett. **142B**, 410 (1984).
[24] M. J. Teper, Phys. Rev. D **59**, 014512 (1998).
[25] M. Caselle, M. Pepe, and A. Rago, J. High Energy Phys. 10 (2004) 005.
[26] M. Caselle, A. Feo, M. Panero, and R. Pellegrini, J. High Energy Phys. 04 (2011) 020.
[27] B. Bringoltz and M. Teper, Phys. Lett. B **645**, 383 (2007).
[28] B. B. Brandt, J. High Energy Phys. 02 (2011) 040.
[29] B. B. Brandt, J. High Energy Phys. 07 (2017) 008.
[30] B. B. Brandt, Proc. Sci. Confinement2018 (**2018**) 039 [arXiv:1811.11779].
[31] B. B. Brandt, arXiv:2102.06413.
[32] O. Philipsen, M. Teper, and H. Wittig, Nucl. Phys. **B469**, 445 (1996).
[33] O. Philipsen, M. Teper, and H. Wittig, Nucl. Phys. **B528**, 379 (1998).
[34] O. Philipsen and H. Wittig, Phys. Rev. Lett. **81**, 4056 (1998); **83**, 2684(E) (1999).
[35] F. Knechtli and R. Sommer (ALPHA Collaboration), Phys. Lett. B **440**, 345 (1998); **454**, 399(E) (1999).
[36] F. Knechtli and R. Sommer (ALPHA Collaboration), Nucl. Phys. **B590**, 309 (2000).
[37] P. W. Stephenson, Nucl. Phys. **B550**, 427 (1999).
[38] O. Philipsen and H. Wittig, Phys. Lett. B **451**, 146 (1999).
[39] S. Kratochvila and P. de Forcrand, Nucl. Phys. **B671**, 103 (2003).
[40] K. Kallio and H. D. Trottier, Phys. Rev. D **66**, 034503 (2002).
[41] M. Pepe and U. J. Wiese, Phys. Rev. Lett. **102**, 191601 (2009).

[42] G. Parisi, R. Petronzio, and F. Rapuano, Phys. Lett. **128B**, 418 (1983).
[43] M. Luscher and P. Weisz, J. High Energy Phys. 09 (2001) 010.
[44] M. Billo, M. Caselle, and R. Pellegrini, J. High Energy Phys. 01 (2012) 104; 04 (2013) 097(E).
[45] M. Luscher and P. Weisz, J. High Energy Phys. 07 (2004) 014.
[46] M. Billo and M. Caselle, J. High Energy Phys. 07 (2005) 038.
[47] M. Billo, M. Caselle, and L. Ferro, J. High Energy Phys. 02 (2006) 070.
[48] M. Billo, M. Caselle, F. Gliozzi, M. Meineri, and R. Pellegrini, J. High Energy Phys. 05 (2012) 130.
[49] O. Aharony and M. Field, J. High Energy Phys. 01 (2011) 065.
[50] A. S. Bakry, M. A. Deliyergiyev, A. A. Galal, A. M. Khalaf, and M. K. William, arXiv:2001.02392.
[51] A. S. Bakry, M. A. Deliyergiyev, A. A. Galal, and M. K. Williams, arXiv:1912.13381.
[52] D. Antonov, L. Del Debbio, and A. Di Giacomo, J. High Energy Phys. 08 (2003) 011.
[53] D. Antonov and A. Di Giacomo, J. High Energy Phys. 03 (2005) 017.